

Technical Memorandum

To: Jeff Uhlmeyer

From: Lauren Gardner, Gonzalo Rada, Gary Elkins and Kevin Senn

cc: Mustafa Mohamedali

Date: May 2020 (original); Revised November 2, 2020

Re. Forensic Desktop Study Report: Montana LTPP Test Sections 30_8129

The Long-Term Pavement Performance (LTPP) Seasonal Monitoring Program (SMP) test section 30_8129¹ was nominated for a desktop study under TPF-5(332) "LTPP Forensic Evaluations." As part of the SMP, the section was instrumented with an on-site weather station and subsurface temperature, moisture, frost detection and water table depth sensors. In addition, during the performance cycle when SMP data collection was active, the collection of falling weight deflectometer (FWD) measurements and downloading of instrumentation data was performed on a monthly interval, and data collection of distress and profile measurements was conducted quarterly (every 3 months). The frequency and types of data collected on this section provides an opportunity to explore the development of fatigue/alligator and transverse cracking in relationship to climatic and other variables. Additionally, as the FWD deflection data exhibit great variation in magnitude, inferences on seasonal load restriction regulations might be developed from this investigation.

SITE DESCRIPTION

LTPP test section 30_8129 is located on U.S. Route 12, eastbound, in Golden Valley County, Montana. U.S. Route 12 is a rural principal arterial with one lane in the direction of traffic. The site is located in a river valley, approximately 500 feet north of the Musselshell River. The difference in elevation between the river and the pavement surface is approximately 10 feet. It is classified as being in a Dry, Freeze climate zone with an average annual precipitation ranging between 8.47 inches (1988) and 18.39 inches (2014). The test section has an average annual freezing index ranging between 387 deg-F deg-days (1999) and 1874 deg-F deg-days (1996). The coordinates of the test section are 46.30759, -109.12174. Photograph 1 shows the test section at Station 0+00 looking eastbound in 2016, while Map 1 shows the geographical location of the test sections relative to Billings, Montana.

¹ First two digits in test section number represent the State Code [30 = Montana]. The final four digits are unique within each State/Province and were assigned at the time the test section was accepted into the LTPP program.

BASELINE PAVEMENT HISTORY

This section of the document presents historical data on the pavement structure and its structural capacity, climate, traffic and pavement distresses.



Photograph 1. LTPP Section 30_8129 at Station 0+00 looking eastbound in 2016.



Map 1. Geographical location of test section relative to Billings, Montana.

Pavement Structure and Construction History

While U.S. Route 12 in Montana was predominantly constructed by 1959, the test section in question was reconstructed and incorporated into the LTPP program in 1988 as part of the GPS-1 Asphalt Concrete on Granular Base Study. Subsequently, the test section was also included as one of the SMP sites in 1992. The pavement structure at the time of its incorporation into the LTPP program consisted of 0.2 inches of chip

seal² and 3 inches of Asphalt Concrete (AC) on 22.8 inches of crushed gravel, granular base over a fine-grained subgrade. The pavement structure for the test section in 1988 is summarized in Table 1; this information corresponds to CONSTRUCTION_NO = 1 (CN = 1) in the LTPP database. No construction events took place during the SMP data collection period (1988 to 2003). A second construction event took place in June 2003 (CN=2) when the pavement section received a shoulder replacement, a 4-inch AC overlay, and a 0.2-inch aggregate seal coat. The pavement structure following this construction event is summarized in Table 2. A final construction event (CN=3) occurred in June 2013; the section received crack sealing and therefore, the overall pavement structure did not change.

Table 1. Pavement structure for CN = 1

Layer Number	Layer Type	Thickness (in.)	Material Code Description
1	Subgrade (untreated)		Fine-Grained Soils: Gravelly Lean Clay with Sand
2	Unbound (granular) base	22.8	Crushed Gravel
3	Asphalt Concrete (AC) Layer	3.0	Hot Mixed, Hot Laid AC, Dense Graded
4	Asphalt Concrete (AC) Layer	0.2	Chip Seal

Table 2. Pavement structure for CN = 2

Layer Number	Layer Type	Thickness (in.)	Material Code Description
1	Subgrade (untreated)		Fine-Grained Soils: Gravelly Lean Clay with Sand
2	Unbound (granular) base	22.8	Crushed Gravel
3	Asphalt Concrete (AC) Layer	3.0	Hot Mixed, Hot Laid AC, Dense Graded
4	Asphalt Concrete (AC) Layer	0.2	Chip Seal
5	Asphalt Concrete (AC) Layer	4.0	Hot Mixed, Hot Laid AC, Dense Graded
6	Asphalt Concrete (AC) Layer	0.2	Seal Coat

Pavement Structural Properties

Figure 1 shows the average FWD deflection under the nominal 9,000-pound load plate over time. This plot shows deflections collected during CN=1 from 1989 to 1997. The deflection of the sensor located in the center of the load plate is a general indication of the total “strength” or response of all layers in the pavement structure to a vertically applied load. Similarly, Figure 2 shows the average deflection 48 inches from the load plate over time. Because of how the FWD (or other) load is distributed on a thin AC pavement, deflections at 48 inches are due almost in their entirety to the subgrade response (i.e., no influence from AC and base layers). As shown in Figures 1 and 2, the deflections observed can be influenced by pavement temperature at the time of testing and moisture conditions. The gravimetric moisture content shown in both figures were calculated from Time Domain Reflectometry (TDR) sensor data collected at a depth of 33 inches below the surface of the pavement, i.e., at the top of the subgrade. The pavement temperature in both figures represents the average daily temperature of the pavement taken at an average depth of 1.85 inches or near the middle of the surface AC layer.

² The use of chip seals on AC overlays is standard practice in Montana DOT as referenced in the State’s Chip Seal Manual.

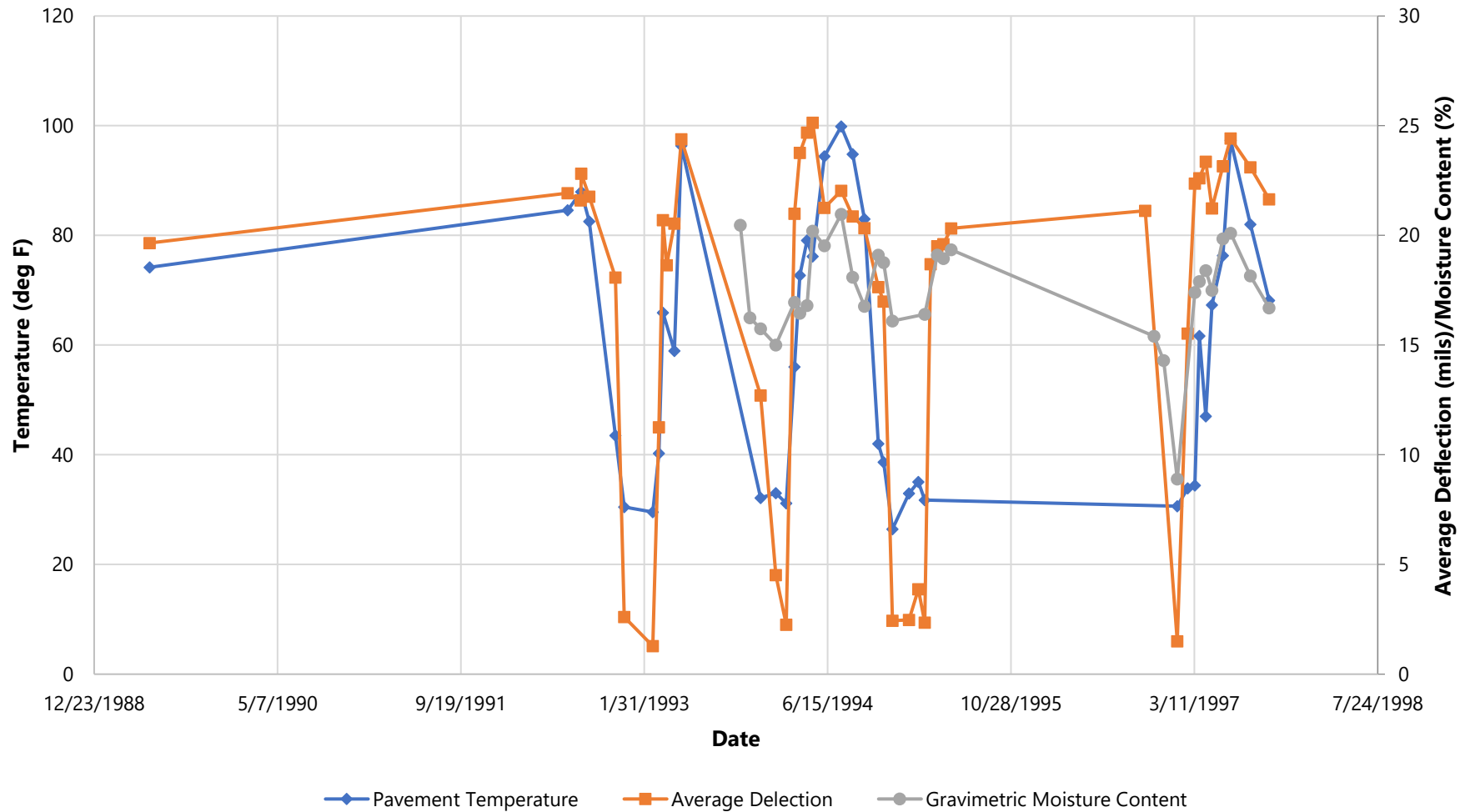


Figure 1. Comparison of a) FWD deflections under the load plate (Sensor 1), b) the average daily temperature of the pavement taken at an average depth of 1.85 inches below the surface, and c) the gravimetric moisture content at a depth of 33 inches below the surface of the pavement (TDR 5).

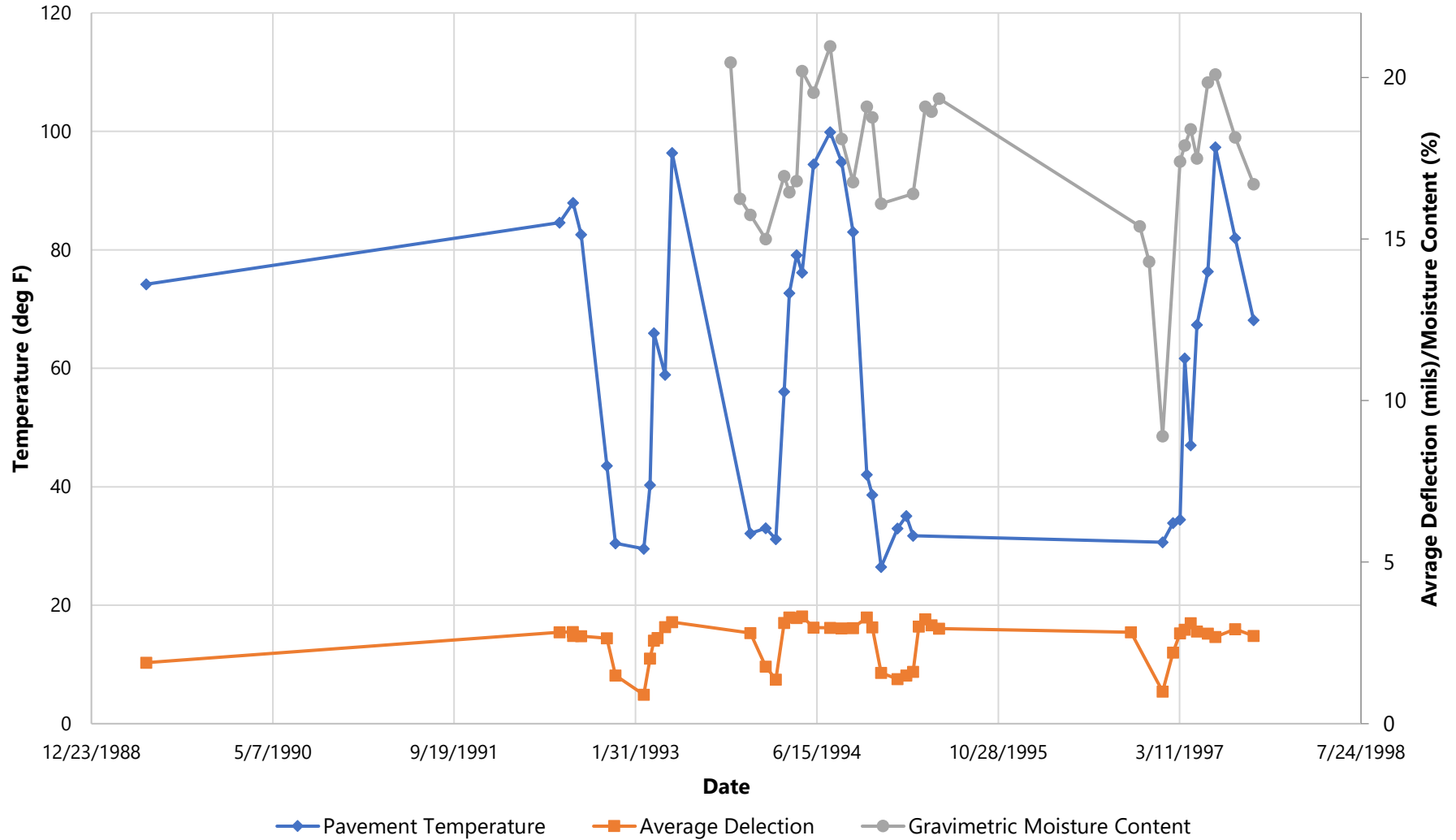


Figure 2. Comparison of a) FWD deflections 48" from the load plate (Sensor 7), b) the average daily temperature of the pavement taken at an average depth of 1.85 inches below the surface, and c) the gravimetric moisture content at a depth of 33 inches below the surface of the pavement (TDR 5).

As depicted in Figures 1 and 2, the change in deflection over time appears to be directly related to the change in pavement temperature and subgrade moisture content over time. For the most part, increases and decreases in deflections correspond to increases and decreases in the pavement temperature and subgrade moisture content. Exceptions include the decrease in average deflection observed in June 1994 despite an increase in pavement temperature and the sharp increase in average deflection observed in March 1995 despite a decrease in pavement temperature; however, in both cases the average deflections increase and decrease as the subgrade moisture content increase or decrease. Another observation that can be made is that, with temperature taken into consideration, the largest increases in deflections observed in Figures 1 and 2 correspond to spring months when it is postulated the subgrade is weakest due to thawing of frost zones. Similarly, the largest decreases in deflections observed correspond to winter months.

Figures 3-6 show the layer moduli backcalculated (using EVERCALC 5.0 software) from the deflection data measured between July 1992 and May 2002. The pavement structure was modeled as a 3-inch AC layer, a 22.8-in granular base layer, the top 24 inches of fine subgrade, and a semi-infinite unbound subgrade layer. One key observation that can be made from figures 3 through 6 is that for the AC, base, and top of subgrade (first 24 inches) layers, there is an abnormal spike in the average modulus reported at the end of 1993 and early 1994. This is likely explained by the frost observed during this period as depicted later in this memorandum in Figure 9. As the frost forms in the inbound pavement layers, the modulus of the layer increases.

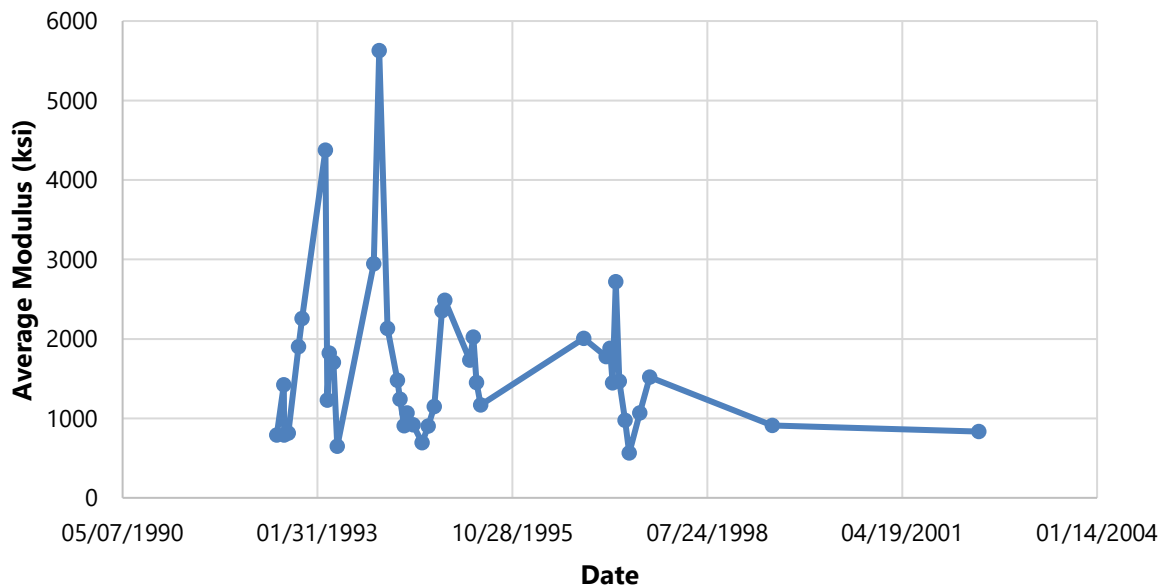


Figure 3. AC layer backcalculated modulus over time.

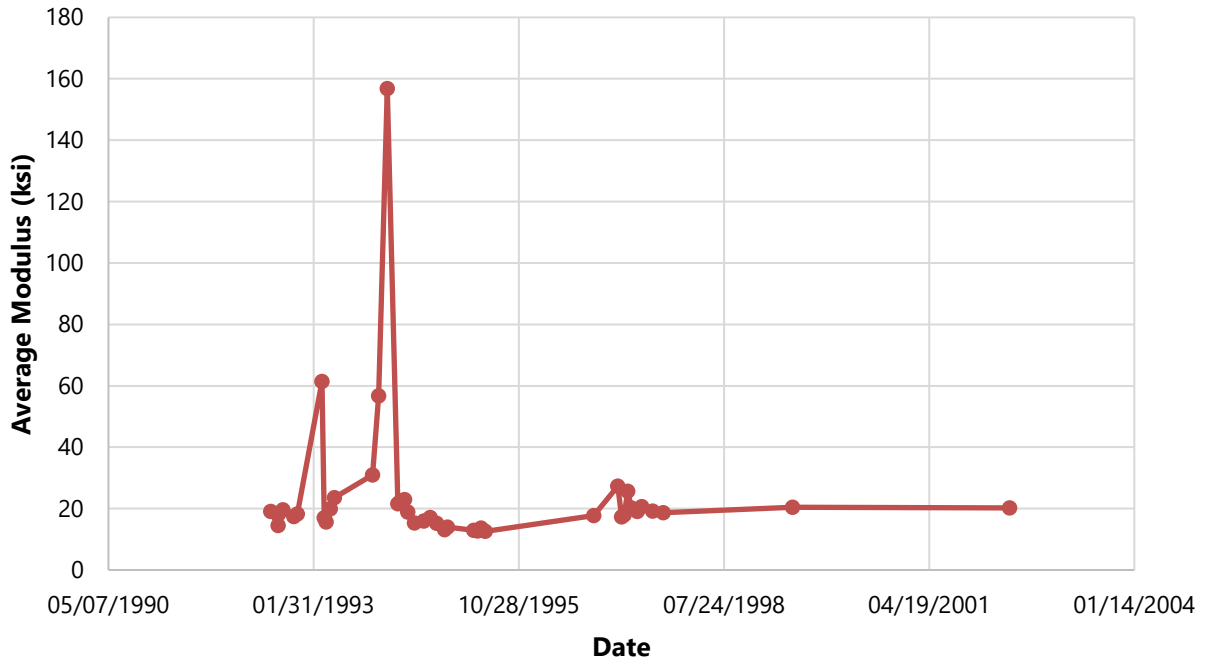
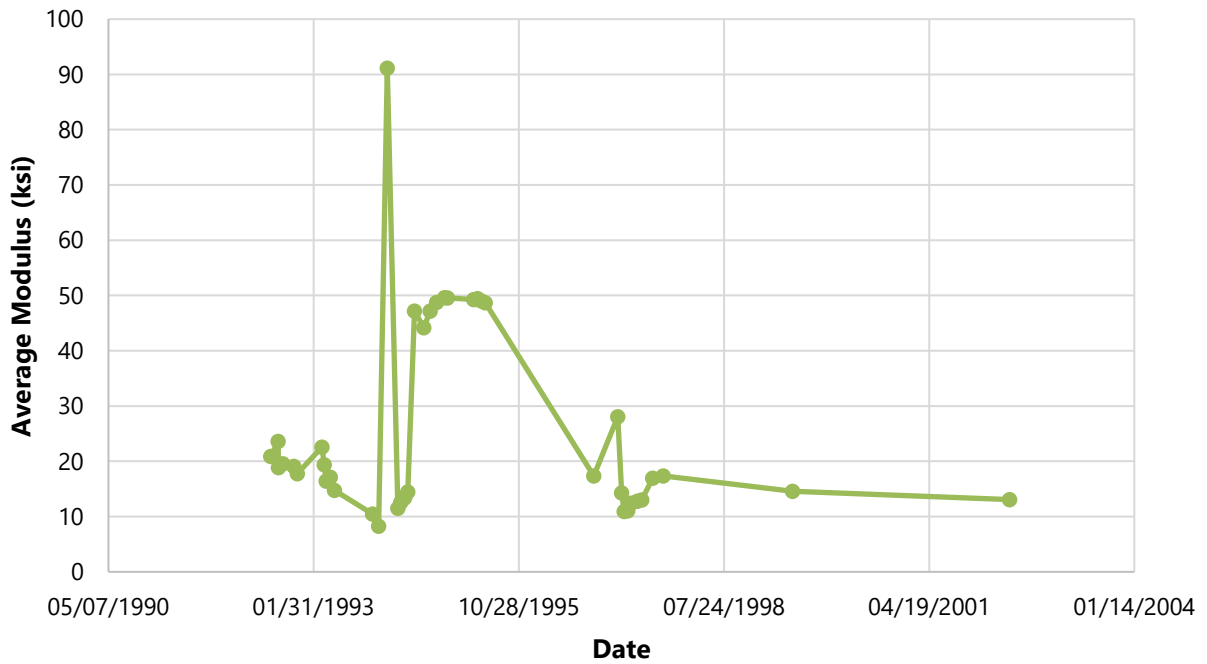


Figure 4. Base layer backcalculated modulus over time.



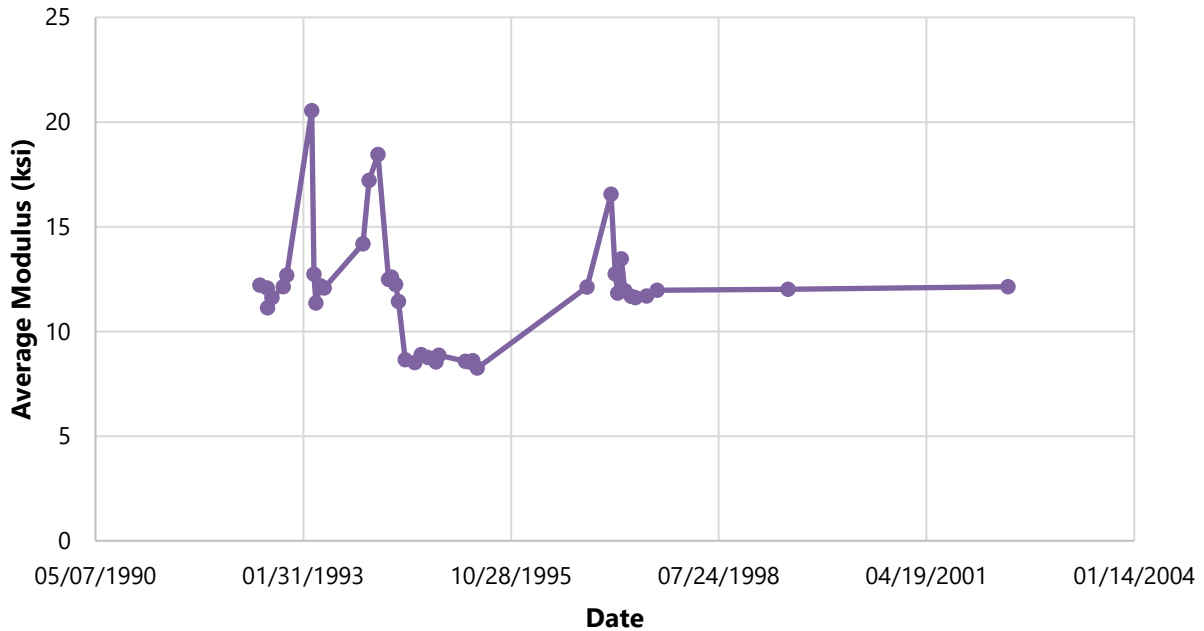


Figure 6. Semi-infinite subgrade layer backcalculated modulus over time.

Deflection Regression Analyses

It was noted in the introduction to this memorandum that since the FWD deflection data at the test section in question exhibits great variation in magnitude, inferences on load restriction regulations might be developed from this investigation. Given the strong relationship between deflections and pavement temperature (at mid-depth of AC surface layer) moisture content (at top of subgrade) and measurement position (FWD sensor location) presented in the previous section, a regression analysis was performed as part of the desktop study to statistically relate variations in deflection to the changes in both the referenced variables and the test section age. It was felt that if a good relationship could be established, then the possibility of developing a deflection-based approach to load restrictions could be obtained through further studies (beyond this LTPP forensic evaluations study).

In this regression analysis, the age variable was calculated by subtracting the test date from the construction date (i.e., 5/31/1988). The position variable was defined as a categorical variable; its value was either 0 for the measurements obtained under the center of the load plate or 1 for the measurements captured at 48" from the load plate. Table 3 shows the results of the regression analysis. As shown, the regression coefficients for pavement temperature and moisture content are positive, which means that if either of these factors increases, the pavement deflections will also increase. In addition, based on the computed p-values, it is apparent that the variation in deflection is highly correlated with temperature, moisture content, and position, while the age of the section was not found to be significant.

The effect of temperature–position and moisture–position interactions on the deflections were also considered. The interaction between two factors is said to occur when the magnitude of the effect of one factor on the dependent variable changes as the level of the other variable changes. Table 3 shows that these interaction effects are statistically significant and that they have a negative effect on the pavement deflection. The impacts of these interactions are shown graphically in Figures 7 and 8. Figure 7 shows that the effect of pavement temperature on deflection is significant for position 0, while it is less significant in

position 1. Similarly, Figure 8 shows that the deflection measurements captured in position 0 are more sensitive to change in moisture content as compared to position 1.

Table 3. Regression analysis results

Factor	Regression Coefficient	P-value
Intercept	17.5350	< 2e-16
Age	0.0013	0.1922
Temperature	0.1507	0.0001
Moisture	1.3102	0.0012
Position	-15.2253	< 2e-16
Temperature * Position	-0.1475	0.0078
Moisture * Position	-1.1414	0.0380

Ultimately, the regression analysis yielded the following model to predict pavement deflection (mils) based on pavement temperature (°F), subgrade moisture content (%), and measurement position (0 or 1):

$$\begin{aligned}
 \text{Deflection} = & 17.95 + 0.15 * (\text{Temperature} - 59.27) + 1.29 * (\text{Moisture Content} - 17.58) - 15.23 \\
 & * \text{Position} - 0.15 * (\text{Temperature} - 59.27) * \text{Position} - 1.14 * (\text{Moisture} - 17.58) \\
 & * \text{Position}
 \end{aligned}$$

At position 0 (under center of load plate), the above equation reduces to:

$$\text{Deflection} = -13.61 + 0.15 * \text{Temperature} + 1.29 * \text{Moisture Content}$$

While at position 1 (48 inches from center of load plate), the equation reduces to:

$$\text{Deflection} = 0.08 + 0.15 * \text{Moisture Content}$$

The scatter plot of the predicted deflection values from the model versus the actual measured deflection values is shown in Figure 9. This plot shows a good correlation between measured and predicted deflection values with a coefficient of determination (R^2) of 0.88. The R^2 shows that 88% variability of deflection data can be explained by the variables in the model.

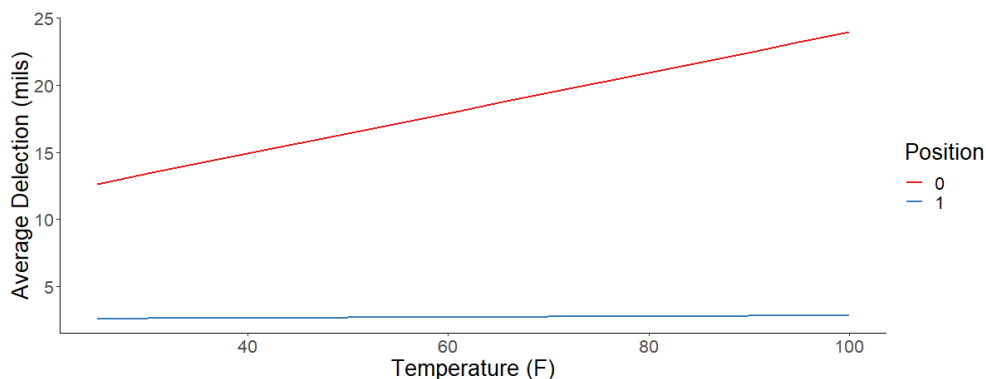


Figure 7. Interaction plot of temperature and position.

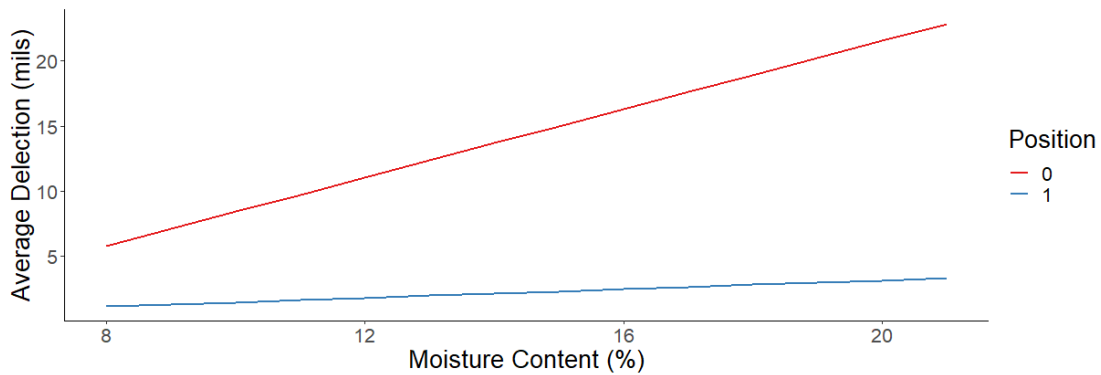


Figure 8. Interaction plot of temperature and position.

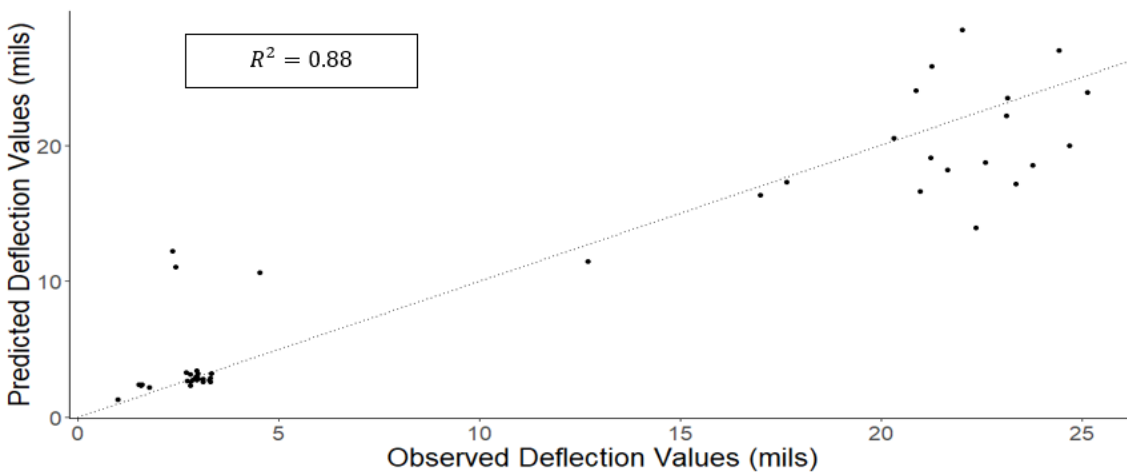


Figure 9. Predicted versus observed values of pavement deflection.

Climate History

The time history for the monthly average precipitation (from the VWS) between 1988 and 2017 is shown in Figure 10. This time history covers more than just CN=1 which was used for the previous part of this investigation. In June 1992, the amount of precipitation is the local high (6.2 inches), while the low (0 inches) was recorded in February 2006. These measurements seem to spike in the spring and summer months (May, June, July, and August) indicating more precipitation occurs during these seasons.

The high levels of precipitation in June 1992, July 1993, and May 2011 may correspond to flooding events at the Musselshell River, just south of the project site. Specifically, the high levels of precipitation observed in May 2011 is likely related to the 150-year flood event. The flood event, which began May 21st, was the result of 8 inches of rain on top of existing snow melt. While the result of the flood event was much worse downstream, the test section may have been impacted by this event and similar high precipitation/flooding events.

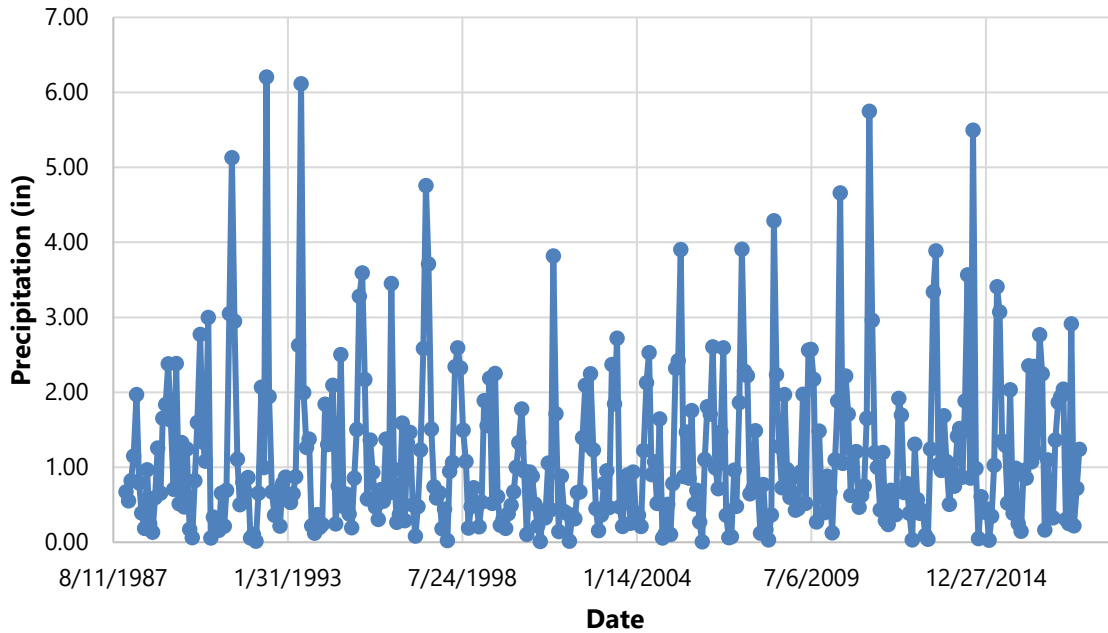


Figure 10. Average monthly precipitation over time.

Figure 11 shows the time history of the average monthly air temperature (from the VWS) over the history of this test section. As shown in Figure 11, the lowest average air temperature (12.7 deg F) occurred in February 1989, while the highest value (74.7 deg F) occurred in July 2017.

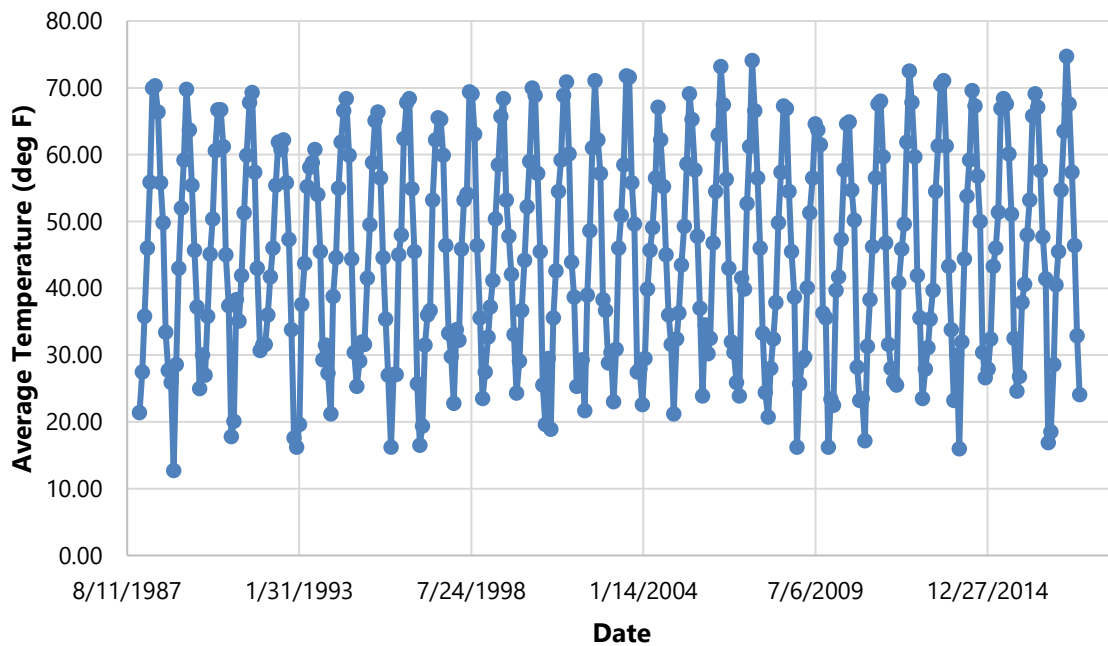


Figure 11. Average monthly air temperature over time.

Figure 12 depicts the average, maximum, and minimum temperature of the material surrounding the site thermistor (Sensor 4) at a depth of 4.68 inches, i.e. near the top of the base layer. The figure is useful in

identifying when the pavement structure is frozen as material temperatures dip below the freezing temperature of 32 degrees Fahrenheit. However, as the figure shows, this only occurs during a small window of the winter months (early December through end of February). In this figure, the very low temperatures observed near the top of the base layer had the lowest recorded temperatures corresponding to the low deflection measurements and high modulus values during the winter of 1993-1994.

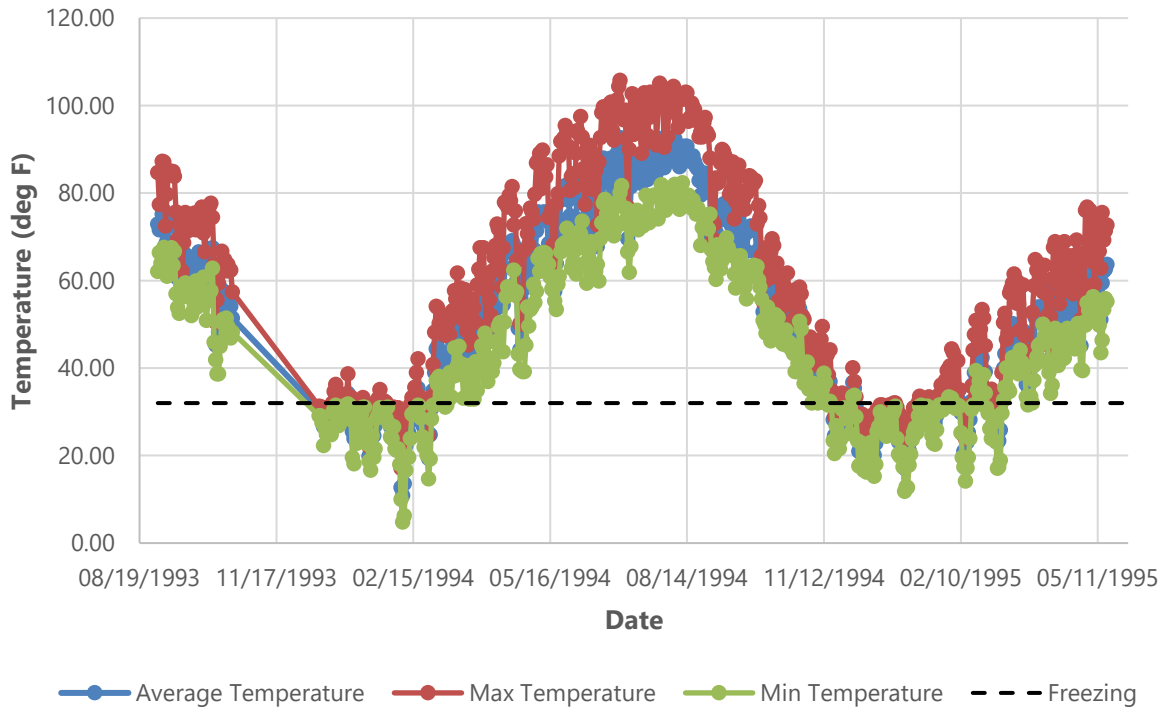


Figure 12. Average, maximum, and minimum temperature of the material surrounding the site thermistor (Sensor 4) at a depth of 4.68 inches.

Truck Volume History

Figure 13 shows the annual average daily truck volume data in the LTPP test lane by year. The annual truck traffic counts increase from 90 in 1988 to 216 in 2017, or approximately 4 additional trucks per year, effectively doubling the truck counts during the period in question. The total annual 18-kip ESALs reported between 2000 and 2013 also increased. The number of 18-kip ESALS increased from 60 in 2000 to 145 in 2013 or by approximately 6.5 18-kip ESALS/year. In terms of either truck or ESAL counts, the traffic at the test section in question is low, which is clearly reflected in the more significant distresses being environment-related (i.e., not load-related) as shown in the next sections.

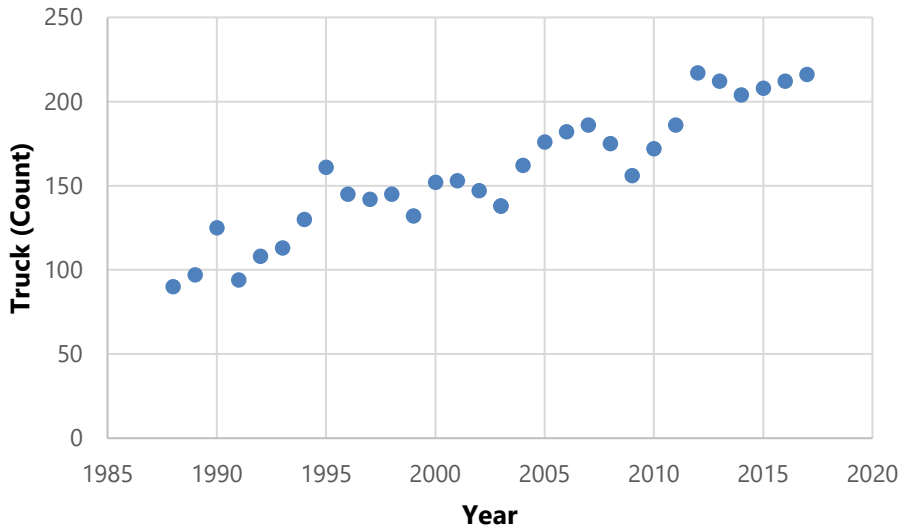


Figure 13. Average annual daily truck traffic (AADTT) history.

Pavement Distress History

The following section summarizes the distresses observed on the test section between the time the section was constructed and 2016, which is when the last manual distress survey was performed. Fatigue/alligator cracking, longitudinal cracking (on and off the wheel path), transverse cracking, IRI, and rutting were reviewed. No block cracking or patching was observed. Fatigue/Alligator Cracking

Fatigue/Alligator Cracking

Figure 14 shows the total area in which fatigue/alligator cracking was observed for the section between 1992 and 2016. While the graph obtained from InfoPave is labeled fatigue cracking, in LTPP low severity wheel path cracking with an area component overlaps with alligator pattern cracks, which are not constrained to the wheel paths. The name fatigue cracking implies a mechanism, whereas the LTPP distress surveyors were reporting only observations of cracking on the surface of the pavement test sections following LTPP guidelines.

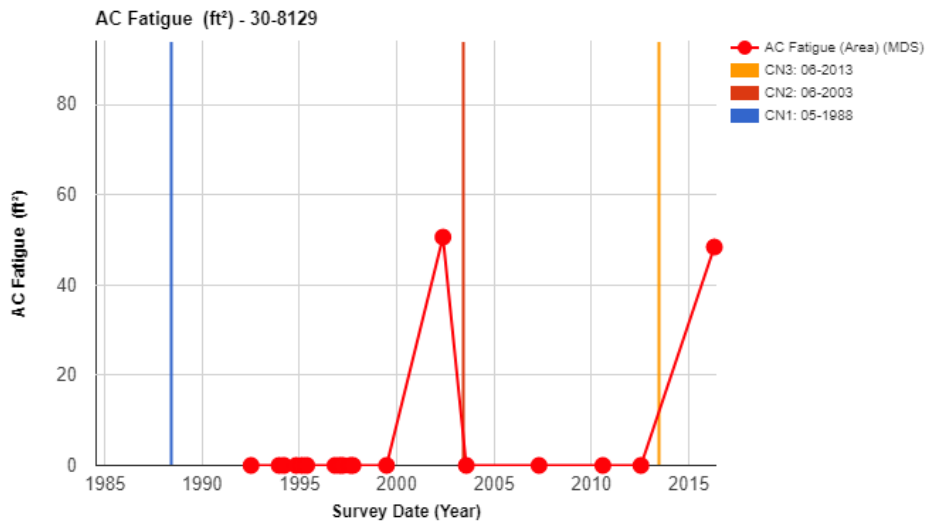


Figure 14. Time history of the area of fatigue/alligator cracks.

No fatigue/alligator cracking was observed on the section between 1992 and 2002. In May 2002, 14 years following CN=1, a total of 50.6 ft² of fatigue/alligator cracking was observed. Fatigue/alligator cracking observed in 2002 was predominantly low severity and within the wheel path. Following the AC overlay in 2003 (CN=2), fatigue/alligator cracking is not observed again for nearly 13 years. It is not until 2016 that 48.6 ft² of fatigue/alligator cracking was observed. Fatigue/alligator cracking observed in 2016 was also predominantly low severity and within the wheel path. However, the location (station numbers) in which fatigue/alligator cracking was observed in 2016 differed from the locations observed in 2002. The increase in fatigue/alligator cracking in 2002 and 2016 parallels the sudden increase in wheel path longitudinal cracking in those same years.

Longitudinal Cracking

Longitudinal cracking, inside and outside the wheel paths of the test section, are defined by LTPP as cracks predominately parallel to the pavement center line and have no detectable area extent. Figure 15 depicts the longitudinal cracking observed in non-wheel path (NWP) portions of the section. The NWP longitudinal cracking observed increased from 344.1 ft in 1992 to 397.9 ft in 2002 or by 5.4 ft/year during the ten-year period or approximately 28.4 ft/year since the initial construction event (CN=1). The longitudinal cracking observed prior to the overlay predominantly occurred at the longitudinal centerline joint of the roadway. Following the AC overlay in 2003, no NWP longitudinal cracking is observed on the section until August 2010, 7 years after the overlay, when 37.1 ft of cracking was observed. By 2016, 13 years after the AC overlay, the NWP longitudinal cracking observed is 158.42 ft. The rate at which longitudinal cracking increases, once initiated, following the overlay is 20.2 ft/year, nearly quadruple the rate of increase observed prior to the overlay. The location of the longitudinal cracking following the overlay is predominantly in-between the two-wheel paths and on the longitudinal joint of the lane, which appears to be reflection cracking.

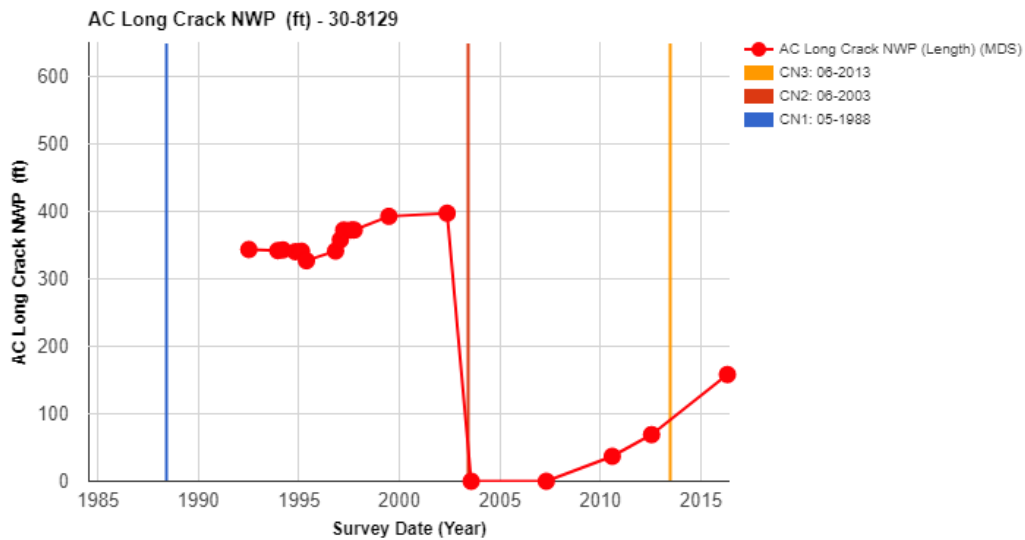


Figure 15. Time history of the length of NWP longitudinal cracks.

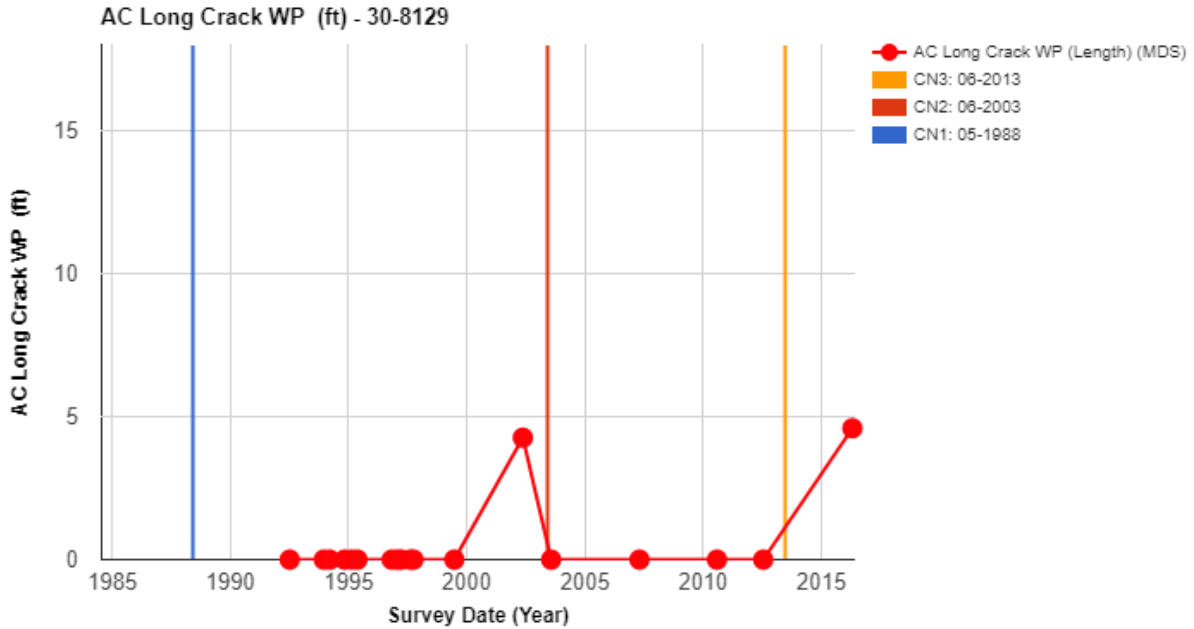


Figure 16. Time history of the length of WP longitudinal cracks.

The longitudinal cracking observed in the wheel path (WP), shown in Figure 16, between the date of the first manual LTPP distress survey (1992) and the date of the last survey before the second construction event remained consistent. Until May 2002, 14 years after CN=1, when 4.3 ft of WP longitudinal cracking was observed, no WP longitudinal cracking was observed on the section. Following the application of the overlay in 2003, no WP longitudinal cracking was observed on the test section until 2016, 13 years after the overlay, when 4.6 ft was observed. The location of the longitudinal cracking observed in the wheel path for the test section differed between 2002 and 2016. The increase in WP longitudinal cracking in 2002 and 2016 parallels the increase in fatigue/alligator cracking in those same years. Despite WP longitudinal cracking being observed in 2002 and 2016, these reported values may be attributed to the inconsistent interpretation of low severity longitudinal cracking within the wheel path and fatigue cracking – fatigue cracking is associated with “random cracking and meandering,” which is difficult to objectively determine in some cases.

Transverse Cracking

Transverse cracking was reported between 1992 and 2016 as shown in Figures 17 and 18. The pavement section reported 195.5 ft on approximately 17 transverse cracks in 1992. By 2002, prior to the AC overlay, 217.1 ft of transverse cracking or approximately 23 cracks were observed on the section. During the 10-year period in which transverse cracking was reported, the cracking increased at a rate of 2.2 ft/year. Following the application of the AC overlay in 2003, transverse cracking does not re-emerge until 2010, 7 years after the overlay, when 36.4 ft (3 cracks) of transverse cracking was observed. By 2016, the year of the last distress survey, 57.4 ft of transverse cracking (13 cracks) was observed. The rate at which transverse cracking propagated, once initiated, following the overlay, was 3.5 ft/year. The location of the transverse cracks reported following the overlay are likely reflected transverse cracks observed prior to the overlay. As depicted in Figure 19, the location of the cracks in 2016 and 2002 are similar, indicating the reflection of transverse cracking after the overlay.

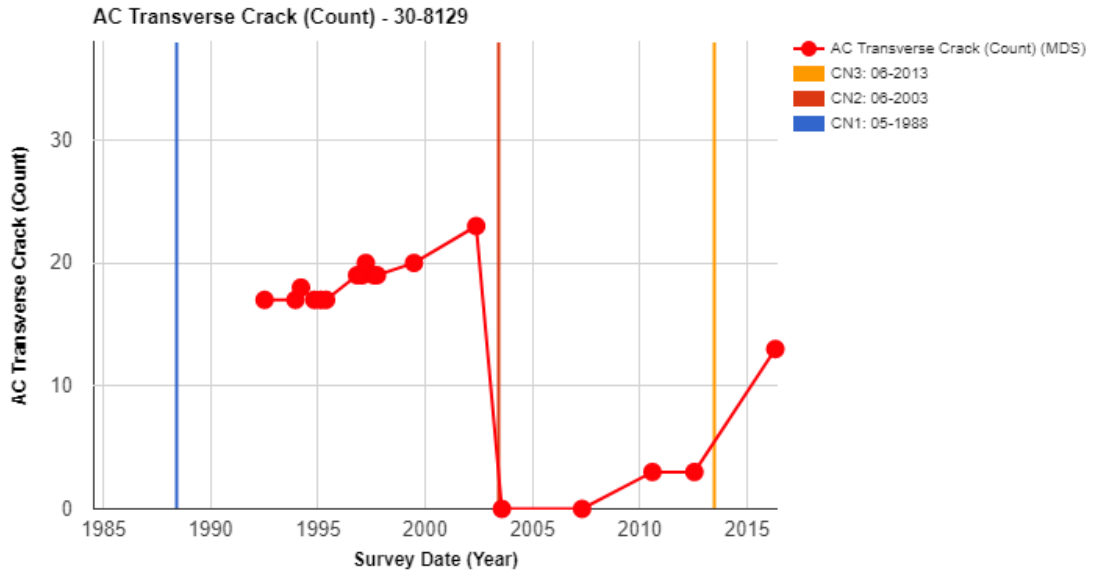


Figure 17. Time history of the number of transverse cracks (count).

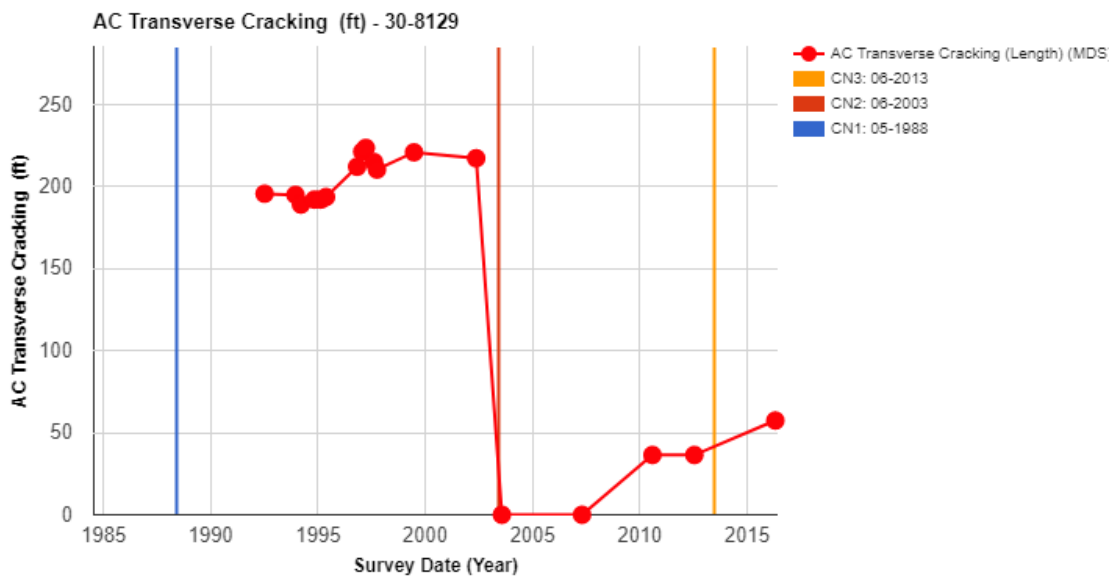
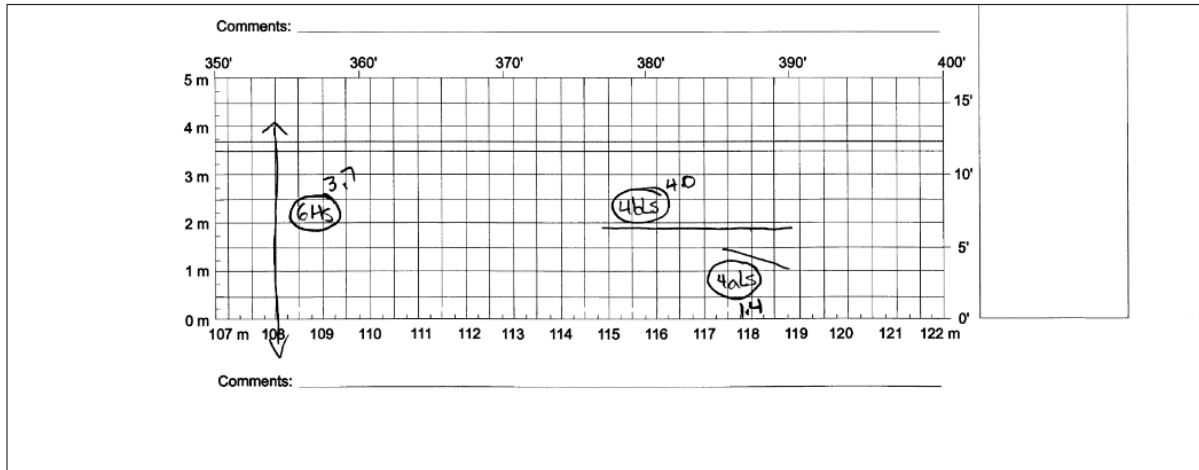


Figure 18. Time history of the length of transverse cracking (length).

Survey Date: 04/25/2016 350 - 400 feet

8/10



Survey Date: 05/17/2002 350 - 400 feet

8/10

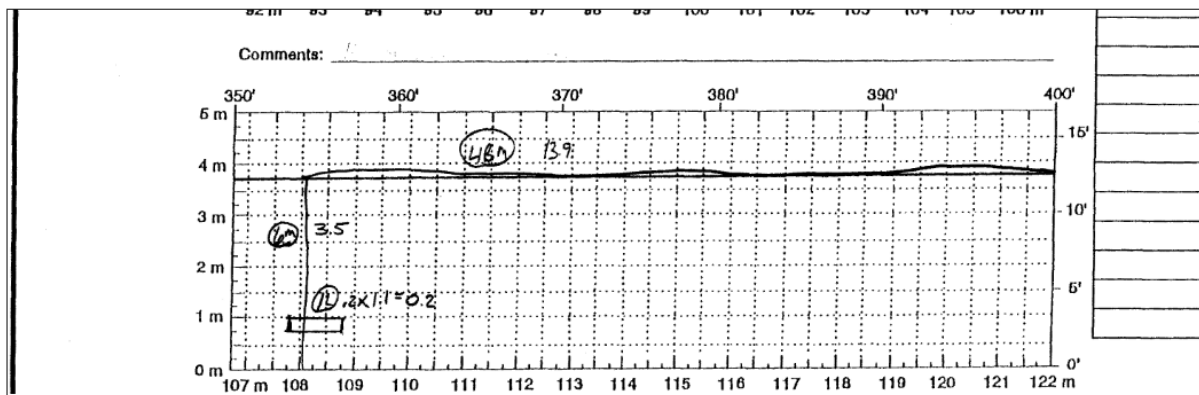


Figure 19. Distress surveys from 2016 (top) and 2002 (bottom) showing transverse cracking in similar locations on the test section between 350 feet and 400 feet from the start station.

The mechanism most often linked to transverse cracking in AC pavements is temperature changes in the AC layer. As discussed previously, the measured pavement temperature (Figure 1) notably varied due to seasonal changes. These variations in temperature likely played a role in the transverse cracking observed on this section. The length of the transverse cracks observed throughout the test section supports this claim. Most of the transverse cracking recorded on the test section was the full width of the lane, indicating low temperature cracking.

IRI

The IRI of the pavement test section, which was calculated from the measured roughness, between 1989 and 2016 is shown in Figure 20. Between 1989 and 2002, the roughness of the test section increased from 53.22 in/mi to 89.4 in/mi, both considered within the Good condition range based on FHWA definitions. While the increase in roughness was gradual prior to the overlay in 2003, the IRI reported on the test section varied slightly based on the time of year which the IRI was reported. In most cases, the roughness of the pavement dropped in colder months (December and January) and increased in warmer months (May, June, July).

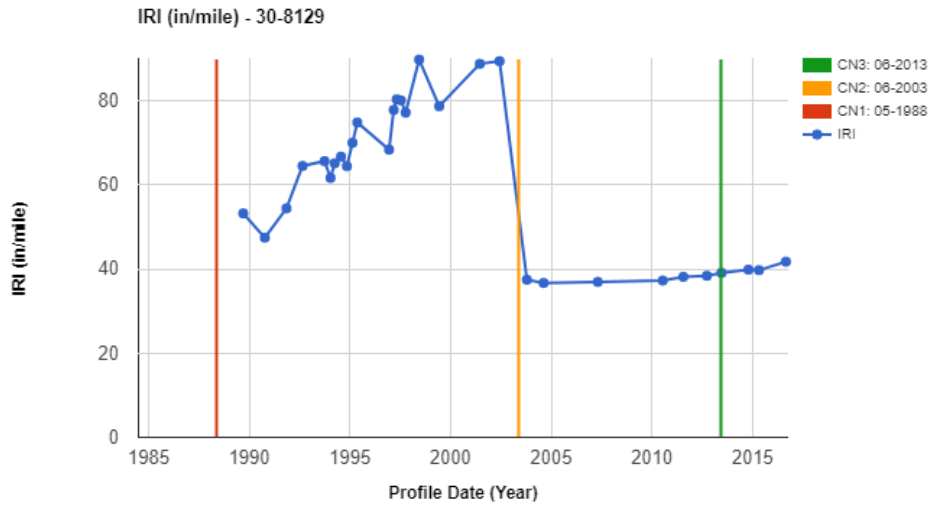


Figure 20. Time history plot of pavement roughness.

Following the application of the AC overlay, reported IRI was more consistent. In October 2003, the roughness reported on the section dropped to 37.5 ft/mi. By 2016, the reported roughness was 41.8 in/mi. Therefore, the increase in IRI value following the AC overlay was 0.3 in/mi/year following the overlay.

Rutting

The rutting observed for the section over time is shown in Figure 21. Between 1988, when the section was accepted, into the study and 2003, when the section received an AC overlay, the rutting steadily increased from 0.35 inches in 1989 to 0.55 in 2002. On average, rut depth increased 0.02 inches/year over a 13-year period. The rutting observed between 1989 and 2002 is aligned with the steady increase in truck traffic during this period. Following the overlay, the rutting observed reduced to 0.08 inches in October 2003. While the average rut depth reported slightly increased in 2007 and 2010, the rut depth reported in 2016 is also 0.08 inches.

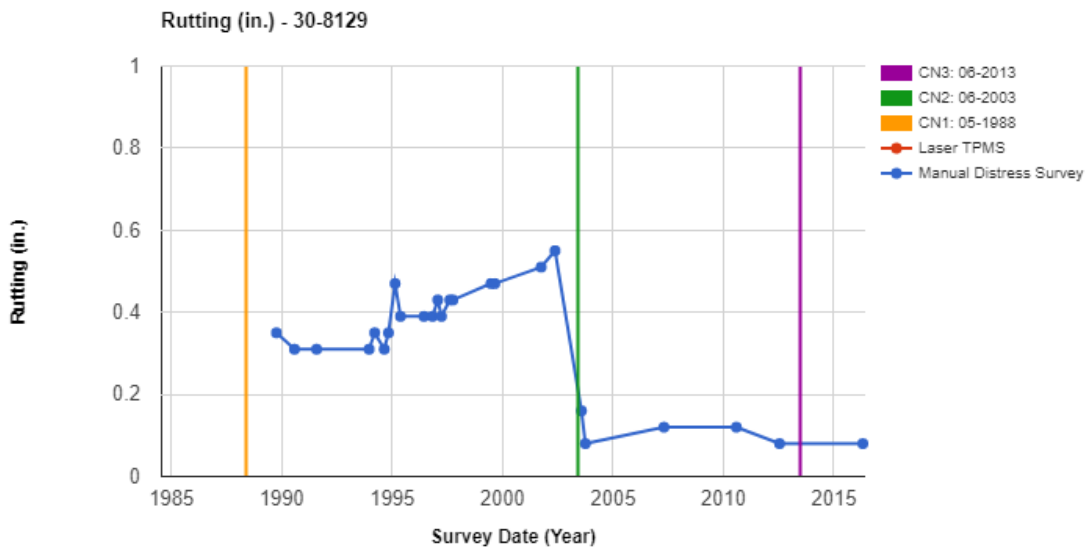


Figure 21. Time history plot of average rut depth computations.

In addition to the average rut depth observed over time, the change in the transverse profile of the test section at station 300 was also investigated. Figure 22 depicts the changes in the profile over time with orange lines representing rutting profiles of the roadway following the overlay in 2003. From the figure, the transverse profiles observed prior to the AC overlay in 2003 show deeper depressions along the wheel path over time. This aligns with the increased average rutting observed over time in Figure 21. Following the overlay in 2003, the normalized elevation is more consistent and closer to level (0 inches).

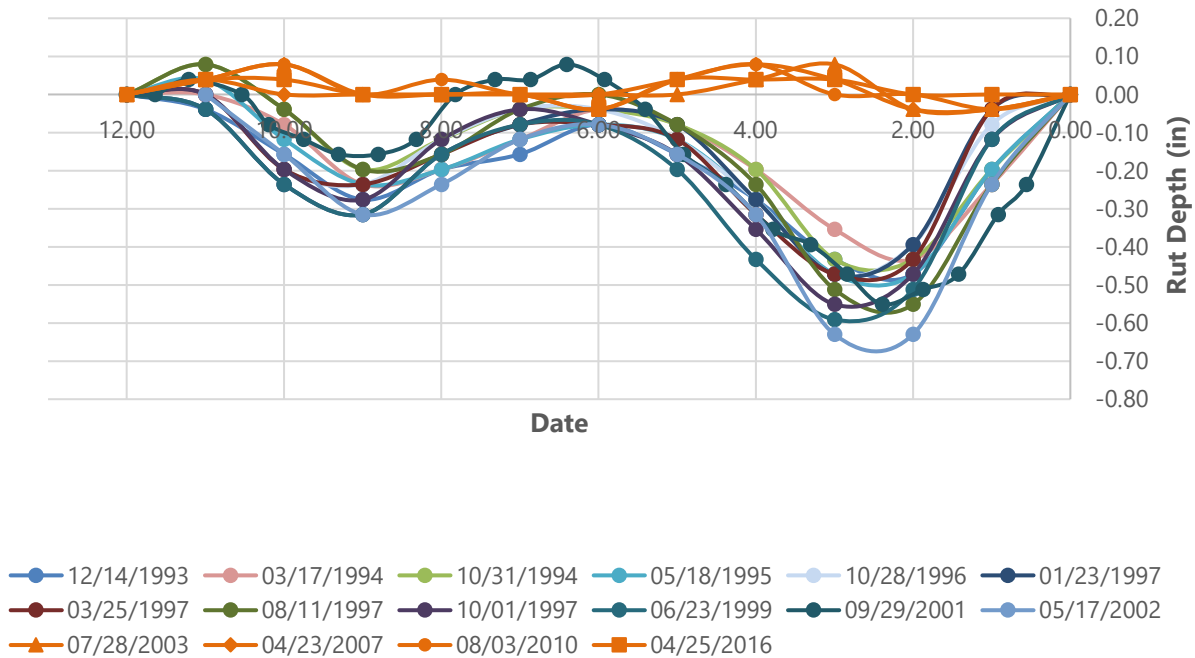


Figure 22. Plot of transverse profile of station 299.79 of transverse profile over time.

Using these same profiles, an analysis of the predominant layer the plastic deformation occurs was assessed using the method developed in NCHRP 01-34a.³ The method, which was derived using finite element analyses of rutting mechanisms in the HMA surface, base, and subgrade, is focused on the transverse profile characteristics indicative of permanent deformation such as densification, shear failure, or shear flow.

The methodology consists of two key steps: calculation of distortion parameters and the use of criteria to classify the lowest layer in the pavement structure contributing to the ruts. Distortion parameters include the maximum rut depth (D), positive area, and negative area of a transverse profile. For each profile, the wire method is used to assess the maximum rut depth, which is the greatest perpendicular distance measured from the pavement surface to the wire reference line as depicted in Figure 23. Similarly, the positive area (A_P) and negative area (A_N) are the sum of the areas above and below the transverse profile reference line, respectively. Using these parameters, the ratio of positive area to negative area (R), total area (A_T), and the theoretical total areas for the HMA, base, and subgrade failure (C_1, C_2 , and C_3 , respectively) are calculated and used to assess the failed layer. The assessment of the parameters used to determine the lowest layer contributing to the pavement's surface deformation is described in Figure 24.

³ White, T., J. Haddock, A.J.T. Hand, & H. Fang. NCHRP 468: *Contributions of Pavement Structural Layers to Rutting of Hot Mix Asphalt Pavements*. National Cooperative Highway Program, Washington D.C., 2002.

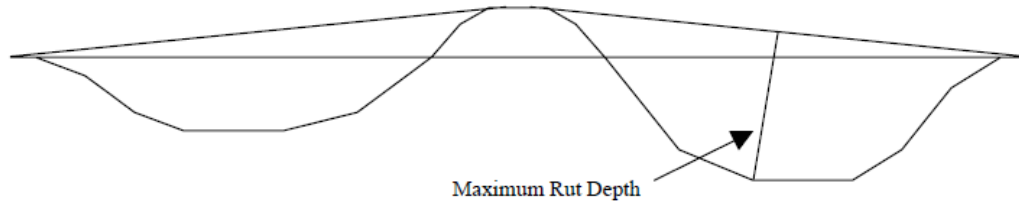


Figure A-1. Definition of maximum rut depth.

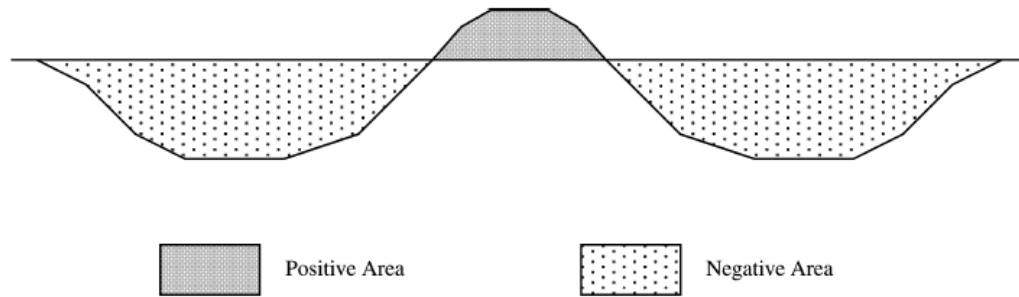
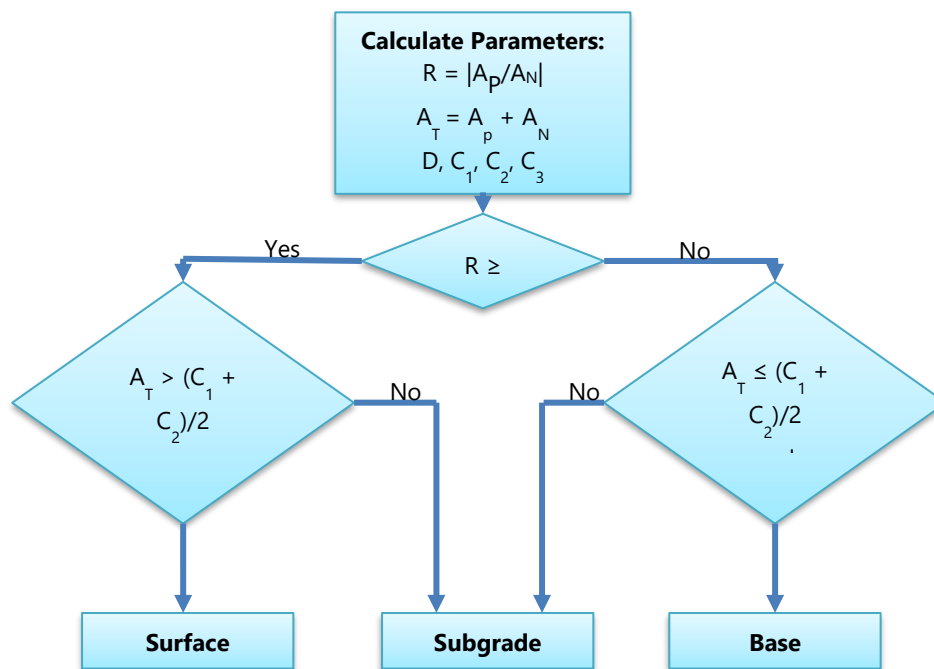


Figure 23. Transverse profile maximum rut depth and positive and negative areas (White et al., 2002)



D= Maximum rut depth
A_p= Positive area (area above pavement surface line of a transverse profile)
A_n= Negative area (area below pavement surface line of a transverse profile)
C₁= (-858.21) D + 667.58, theoretical total area for HMA failure
C₂= (-1509) D - 287.78, theoretical average total for base/subbase failure
C₃= (-2120.1) D - 407.95, theoretical average for subgrade failure

Figure 24. Failure layer determination using methodology by White et al. (2002)

Based on the analysis conducted for each of the transverse profiles in Figure 22, the lowest layer contributing to rutting was calculated for each date of collection. Except for September 2001 (where the surface layer was the lowest layer contributing to rutting), the lowest layer contributing to rutting prior to overlay in 2003 was the base layer. Following the overlay in 2003, the lowest layer contributing to rutting was found to be the surface layer. Based on both the findings of the analysis and the transverse profiles, rutting appears to be due to permanent deformation rather than ablative wear of the pavement surface due to vehicle traction devices, i.e. chains and studded tires.

SUMMARY OF FINDINGS

In this review of information concerning the performance history of test section 30_8129, the following information was presented:

- **Pavement structure history:** The test section was originally constructed in 1988 and at the time of its incorporation into the LTPP program, the pavement consisted of a 0.2 inch of chip seal and 3 inches of AC on 22.8 inches of granular base (crushed gravel) over a fine-grained subgrade. The section was incorporated into the LTPP program in 1988 as part of the GPS-1 Asphalt Concrete on Granular Base Study. Subsequently, the test section was also included as a SMP site in 1992. A second construction event took place in June 2003 (CN=2), when the pavement section received a shoulder replacement, a 4-inch AC overlay, and a 0.2-inch aggregate seal coat. A final construction event (CN=3) occurred in June 2013, when the section received crack sealing.
- **Average deflection under load plate:** In this study, the average deflection observed over time when it was monitored under the SMP was reviewed to associate deflections with climate changes related to seasonal temperature and moisture fluctuations. The deflections observed fluctuated greatly based on the seasonal variation. Specifically, the change in deflection appeared to be related to the changes in pavement temperature and subgrade moisture content over time. For the most part, increases and decreases in deflections corresponded to increases and decreases in the pavement temperature and subgrade moisture content. Moreover, a regression to predict deflections as a function of pavement temperature, moisture content and FWD sensor location was successfully developed, which may enable the use of deflection testing as a means of establishing load restrictions during the spring-thaw period.
- **Pavement distresses:** A summary of the pavement distresses (fatigue/alligator cracking, WP and NWP longitudinal cracking, transverse cracking, IRI, and rutting) observed on the section before and after the overlay event in 2003 is presented in Table 4. As shown in this table:
 - Minimal fatigue/alligator and longitudinal cracking within the wheel path were observed on the section. The distresses were not observed until 14 years after the reconstruction date (1988) and 13 years after the overlay event in 2003.
 - Longitudinal NWP cracking was observed in 1992, the first year a distress survey was conducted on the section, and propagated at a rate of 5.4 ft/year during the ten-period prior to the overlay in 2003. This crack occurred at the pavement centreline longitudinal joint of this two lane highway. Following the overlay, cracking initiation began in 2010, or 7 years after the overlay event, and propagated at a rate of 20 ft/year.
 - Transverse cracking was observed during the first distress survey taken of the section in 1992 and propagated at a rate of 2.2 ft/year prior to the overlay. Following the overlay, crack initiation began in 2010, or 7 years after the overlay, and propagated at a rate of 3.5 ft/year. Low temperature cracking and reflection cracking appears to have played a role in the transverse cracking observed on this section.

- o IRI observed on the section prior to the 2003 overlay increased from 53.22 in/mi in 1989 to 89.4 in/mi in 2002 or at a rate of 2.78 in/mi/year. Following the overlay, the IRI dropped to 37.45 in/mi in 2003 and increased to 41.75 in/mi by 2016, propagating at a rate of 0.33 in/mi/year. It is worth noting that while there was significant transverse cracking, the stated level of IRI was in the excellent to good range.
- o The rutting observed on the section steadily increased from 0.35 in in 1989 to 0.55 in 2002 or 0.02 inches/year over the 13-year period. The rutting observed between 1989 and 2002 is aligned with the steady increase in truck traffic during this period. Following the overlay, the rutting observed decreased to 0.08 inches in October 2003. While the average rut depth reported slightly increased in 2007 and 2010, the rut depth reported in 2016 was also 0.08 in. Using the method defined in NCHRP 01-34a, the lowest layer contributing to rutting for station 300 prior to overlay in 2003 (with the exception of the 2001 profile) was the base layer. Following the overlay in 2003, the lowest layer contributing to rutting was found to be the surface layer. Based on both the findings of the analysis and the transverse profile itself, rutting appears to be due to permanent deformation rather than ablative surface wear due to vehicle traction devices like chains and studded tires.

Considering the information gathered and analyses performed, it appears that adequate data are available in the LTPP database to characterize the performance of the test section in terms of the various measures considered in the analysis. Based on the analysis conducted, the change in deflection over time appears to be directly related to the daily and seasonal change in pavement temperature and subgrade moisture content over time. For the most part, increases and decreases in deflections correspond to increases and decreases in the pavement temperature and subgrade moisture content. While a broader study of other projects is necessary, these findings can be useful in developing load restriction regulations. Additionally, it was found that climatic factors did not play the same role for pavement distresses as they did for pavement deflection. While some pavement distresses increased over time, the rate of propagation was gradual and did not seem to vary greatly despite the fluctuation in climatic factors over time.

Table 4. Test section attribute summary

Attribute	Before Overlay in 2003		After Overlay in 2003	
	First Year Distress Observed	Last Year Distress Observed	First Year Distress Observed	Last Year Distress Observed
Fatigue/Alligator cracking (ft ²)	50.60 (in 2002)	-	48.60 (in 2016)	-
Longitudinal WP Cracking (ft)	4.26 (in 2002)	-	4.59 (in 2016)	-
Longitudinal NWP Cracking (ft)	344.07 (in 1992)	397.86 (in 2002)	37.06 (in 2010)	158.42 (in 2016)
Transverse Cracking	195.50 ft or 17 cracks (in 1992)	217.10 ft or 23 cracks (in 2002)	36.40 ft or 3 cracks (in 2010)	57.40 ft or 13 cracks (in 2016)
IRI (in/mi)	53.22 (in 1989)	89.4 (in 2002)	37.45 (in 2003)	41.75 (in 2016)
Rutting (in)	0.35 (in 1989)	0.55 (in 2002)	0.08 (in 2003)	0.08 (in 2016)

FUTURE RECOMMENDATIONS

Based on the information gathered and analysed in the above sections, only close-out monitoring (pavement surface distress survey, longitudinal and transverse profile surveys, and deflection testing) is recommended at this time in terms of new data collection. It is further recommended that the use of deflection-based regressions be further pursued (i.e., explore at other sites) as a means for establishing spring-thaw load restrictions – this could be started as part of the pooled fund study in question and then further developed under the FHWA LTPP program. In addition, if the Montana DOT is willing to support the pooled fund study, it would be ideal if coring is performed at the test section to verify layer thicknesses and to further investigate the permanent deformation of the pavement layers.

